3.5 GHZ ESC SENSOR TEST APPARATUS USING FIELD-MEASURED WAVEFORMS

Raied Caromi, John Mink, Cosburn Wedderburn, Michael Souryal, and Naceur El Ouni

National Institute of Standards and Technology, Gaithersburg, Maryland, U.S.

ABSTRACT

This paper presents an approach and apparatus for laboratory evaluation of environmental sensing capability (ESC) sensors for the 3.5 GHz band. These sensors are designed to detect federal incumbent signals in the band so that the incumbent can be dynamically protected from harmful interference. The proposed approach is unique in that it utilizes waveforms captured in the field to reproduce in a controlled laboratory environment what the sensor would experience in the field, and with repeatability unattainable in live field testing. Test signals comprise the incumbent signal to be detected, co-channel commercial signals, and the out-of-band emissions of adjacent-band incumbents, including channel propagation effects that can affect sensor performance. We describe an implementation of this approach in software-controlled instrumentation for automated testing of large numbers of test waveforms capable of producing statistically significant performance metrics such as rates of detection and false alarm in a time efficient manner. The material described in this paper is based on research conducted at the National Institute of Standards and Technology and is not related to any certification testing of ESC sensors.

1 INTRODUCTION

The Citizens Broadband Radio Service (CBRS) in the United States permits commercial broadband access to the radiofrequency spectrum between 3550 MHz and 3700 MHz (3.5 GHz band) on a shared basis with existing incumbents in the band [1]. Among the incumbents is the U.S. military which operates radar systems in this band, including shipborne radar off the U.S. coasts. The CBRS rules permit dynamic access to the band in the proximity of military radar provided a sensor network detects the presence of incumbent radar and triggers interference mitigation measures when necessary. The scope of this paper is the quantitative evaluation of the detection performance of these sensors.

In order to operate in the CBRS ecosystem, sensors must meet specific requirements. Among these requirements is the ability to detect the in-band incumbent radar signal at a minimum received power density of −89 dBm (dB relative to 1 mW)/MHz [2], within 60 s of onset, and with a probability of detection of 99 % or better [3].[1] With this minimum required power density, the detection is clearly not thermal-noise-limited, as the detection threshold is 25 dB above the thermal noise floor. The challenge for detection is presented, rather, by co-channel interference.

[1]Government requirements do not specify a maximum probability of false alarm, although this figure of merit is of interest to commercial users.

There are two primary sources of co-channel interference at the sensor's receiver. First, by design, the band is shared with commercial systems. Therefore, sensors must be able to detect the incumbent signal in channels occupied by commercial systems. These systems are expected to be fourth-generation time-division-duplex (TDD) long term evolution (LTE) systems, at least initially. However, the emissions of commercial systems operating in the band can, in principle, be controlled by treating the sensors as protected entities in the CBRS system.

The second, more challenging, source of interference is the out-of-band emissions of systems operating in adjacent bands. These systems are also military radars, operate at frequencies below the CBRS band, and have been observed to generate significant emissions into the CBRS band [4, 5].

This paper presents a testing approach and apparatus that utilizes field-measured waveforms of emissions in the 3.5 GHz band to verify that a sensor meets the requirements for federal incumbent detection. It leverages an extensive library of high-resolution digital recordings of emissions collected by the National Advanced Spectrum Communications and Test Network (NASCTN) [4, 5] to reproduce in a controlled laboratory environment what a sensor would "see" in the field from offshore radars currently operating in the band as well as the out-of-band emissions from adjacent-band radars that can potentially interfere with the in-band signals of interest.

There are several advantages of using field-measured waveforms for laboratory testing. First, because they were recorded by instruments mounted in locations similar to where sensors will eventually be deployed, they represent the channel propagation and other effects that signals received by the sensors will experience, such as tropospheric scatter and time-varying multipath fading, which can distort the transmitted radar signal. Second, these waveforms can be scaled and combined with other signals expected to be present in the band, such as commercial LTE signals, to produce a wide range of scenarios including multiple co-incident radar signals and a multitude of different frequency and amplitude offsets between these signals. Third, the waveforms can be generated by calibrated instrumentation with a degree of repeatability unattainable in live field testing. Finally, the framework is extensible to include additional signals not currently operating but anticipated to operate in the band.

The remainder of the paper is organized as follows. Section 2 reviews the current testing approach and contrasts it with the proposed approach. After providing an overview of the test system in Section 3, we describe the major sub-systems including pre-testing waveform generation (Section 4) and the test harness itself (Section 5) which automates signal generation and sensor notification logging. The paper concludes in Section 6 with several examples of practical test scenarios generated by the test harness.

2 BACKGROUND AND MOTIVATION

2.1 Prior Work

Procedures and waveforms for certification testing of the first commercial environmental sensing capability (ESC) systems are documented in [2]. These procedures are intended to evaluate the ability of an ESC sensor to meet established detection requirements in a laboratory environment, prior to field testing and deployment. The test plan describes five categories of radar pulse waveforms that represent current and future radars in the CBRS band. Each category specifies a pulse modulation type and a range of values for several parameters of the pulse, including pulse duration, pulse repetition rate, and chirp width (if applicable). Tests will expose the sensor to bursts of pulses of each category, with parameter values selected randomly from the given ranges, and will record positive detections. A signal generator will inject the radio frequency (RF) radar pulse waveforms into the sensor under test. The test signals will be conducted if the sensor supports a direct RF cable connection, or radiated otherwise.

In deployment, ESC sensors will be required to detect federal incumbent signals in the presence of background noise from commercial CBRS devices (CBSDs), such as LTE small cells, operating in the band. The laboratory test procedures outlined in [2] specify that Gaussian noise will be added to the radar pulse waveforms to represent the background signal. The test plan mentions that consideration will be given to the out-of-band emissions from adjacent-band radars into the CBRS band, but it does not provide procedures for quantitatively assessing a sensor's ability to detect in-band radar in the presence of these emissions. Furthermore, the test plan omits consideration of channel propagation effects, such as multipath fading, which can distort the transmitted radar pulse waveforms.

2.2 Field-Measured Waveforms

This paper builds on the work in [2] and proposes procedures for evaluating ESC sensors using pre-recorded waveforms measured in the field. We propose to use such field-measured waveforms, in conjunction with simulated waveforms of commercial devices that will enter the band as well as signal processing that models channel effects, to create test waveforms that are more reflective of the signals these sensors will receive in real-world deployments.

Field measurements of the incumbent radar currently operating in the CBRS band were conducted at two U.S. coastal locations over a period of two months at each location [4, 5]. The outcome of these measurement campaigns is an extensive library of radar pulse waveforms in the form of in-phase and quadrature (I/Q) samples spanning an instantaneous acquisition bandwidth of $200\,\mathrm{MHz}$. Each acquisition is continuously sampled at $225\,\mathrm{MSa}$ (megasample)$/\mathrm{s}$ for a duration of $60\,\mathrm{s}$.

The measurements were collected at coastal locations and with antenna heights similar to what a deployed ESC sensor may use. The recorded waveforms, therefore, include the channel propagation effects the received signals would likely experience in practice. In addition to the in-band radar, the measurements include recordings of the out-of-band emissions (OOBE) of adjacent-band radars, both coincident with and in the absence of the in-band radar. The test procedures described below make use of these out-of-band emissions to form the background signal received by the sensor under test.

3 SYSTEM OVERVIEW

The proposed ESC testing system utilizes field-measured signals of both incumbent radar and OOBE of adjacent-band radars. In addition, generated LTE signals with fading channel effects (or measured LTE signals) can be added. In contrast, the current ESC testing procedure adds white gaussian noise (WGN) as interference based on the assumption that the aggregate LTE signals from CBSDs can be represented by WGN [2]. However, certain operating scenarios may result in an interference signal that includes one dominant LTE signal. Unlike WGN, an LTE signal has structure; the shape of its power spectrum is not flat and is subject to the LTE signal configuration. Additionally, channel fading will further affect the LTE signal. Therefore, we consider the scenario in which one LTE signal is dominant in addition to the WGN case.

The test allows for one or more incumbent radar signals with different combinations of interference signals. Since the original field-measured waveforms are $60\,\mathrm{s}$ long, we choose $90\,\mathrm{s}$ for the generated test files. This configuration provides the possibility for starting the radar signal at a random time in the test with some constraints. Specifically, we limit the incumbent radar signal start time to values between $4\,\mathrm{s}$ and $30\,\mathrm{s}$. The start time randomization is important for measuring the latency between the actual radar signal appearance and its reported detection time. Additionally, if the sensor reports a detection before the radar signal appears, the test harness can log a false alarm. Furthermore, waveforms with no incumbent radar signals and similar interference power levels can be generated to test for the probability of false alarm. These waveforms are generated with the $3.5\,\mathrm{GHz}$ waveform generator software tool [6] as shown in Fig. 1. The waveform generator also logs the waveform generation parameters including instantaneous measurements of the signal to interference ratio (SIR). The parameters can be used for fine tuning

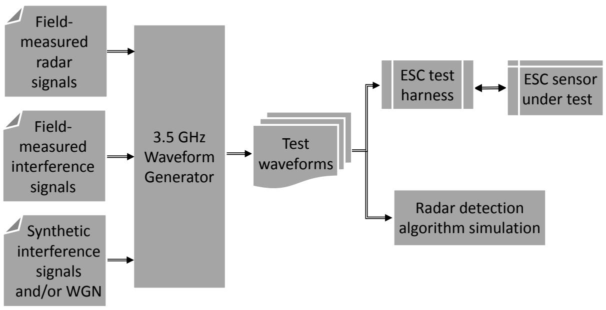

Figure 1: ESC testing system overview

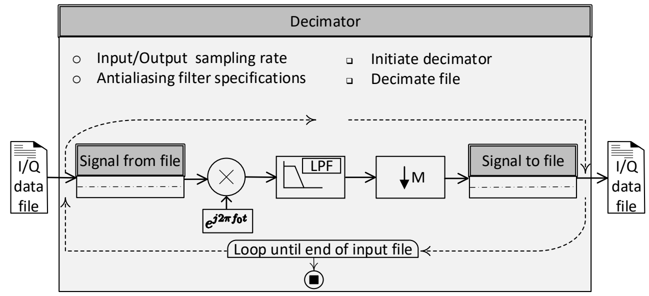

Figure 2: Radar source waveform decimation with a low-pass filter (LPF)

the selection of waveform files for a specific test. They are also used in post-processing to calculate performance metrics.

The selected waveforms are fed to the ESC test harness which consists of a control logic unit, an RF playback device, and RF recording device. The control logic unit is responsible for organizing the flow of the test and logging the test results. It first sends the appropriate file and some additional playback parameters to the RF playback device. Then, it monitors when the playback of each file finishes, listens to a response from the ESC sensor under test, logs the test metadata, and sends the next file to the RF playback device. The test finishes when all the files in a list of selected files are played. Alternatively, the waveforms can be used for development of ESC detection algorithms without RF playback. Throughout this paper, we use a sampling rate of $25\,\mathrm{MHz}$ for all the generated waveforms with effective bandwidth of $20\,\mathrm{MHz}$. This configuration enables us to include up to two $10\,\mathrm{MHz}$ LTE signals with no overlap in the frequency domain.

4 WAVEFORM GENERATION

A waveform generator software tool handles the process of generating the RF playback waveforms [6, 7]. The waveform generator utilizes the field-measured waveforms to generate multiple testing scenarios in which one or more radars operate in the presence of interference such as LTE signals and adjacent-band radar emissions. The waveform generator consists of a signal input/output framework, signal processing procedures, and a graphical user interface (GUI). The signal input/output framework handles the process of reading and writing the signals from/to signal files. All signals are saved as 16-bit integer interleaved in-phase/quadrature (I/Q) data files with appropriate scaling. The reading, writing, and signal processing procedures are performed in terms of segments of samples. The framework also handles the tracking of signal timing and multi-task process execution.

4.1 Signal Preprocessing and Measurement Preparations

Certain tasks are performed prior to the waveform generation process. Specifically, the field-measured waveforms are decimated from $225\,\mathrm{MHz}$ to $25\,\mathrm{MHz}$ sampling rate and an anti-aliasing low-pass filter is applied to the waveform. The waveforms are shifted with an appropriate frequency for each waveform to center the radar signal at zero Hz baseband. The decimation process is preformed in parallel to reduce the run time when processing multiple files. Fig. 2 demonstrates the decimation process with its attributes and tasks for one waveform. In addition, the instantaneous signal to interference ratio (SIR) calculation performed during the generation process requires estimation of radar peak amplitudes and their times for every rotation of the radar antenna. The peak estimation is performed on the all selected waveforms before the generation process.

In addition to the adjacent-band interference (ABI) signals, we generate waveforms that incorporate LTE interference signals. Specifically, TDD LTE signals are simulated and upsampled to the final waveform sampling rate in advance. These signals represent the case when one LTE signal per CBRS channel is dominant at the ESC receiver. Furthermore, captured LTE TDD signals with more realistic out-of-band characteristics can be used instead of computer-generated LTE signals.

4.2 Waveform Generator

Fig. 3 shows the generation process of one waveform with all the required attributes and tasks. The attributes define the characteristics of the waveform, while the tasks control the generation process. A single waveform consists of one or more radar and interference signals. For radar signals, the output waveforms from Fig. 2 are used as inputs to the waveform of Fig. 3. Each signal in the waveform has attributes such as status, center frequency in the baseband, start time, and channel effect for LTE signals. The gain for each signal is estimated from either the desired power signal power level, or the desired SIR. A higher level object in the framework controls the process of generating multiple waveforms. Specifically, the waveform generator object randomizes certain parameters for each waveform such signal start time, frequency, and SIR. Furthermore, it automates and parallelizes the generation process of these waveforms.

In addition, we develop a GUI to visualize the resulting waveforms and simplify the selection of waveform parameters. The

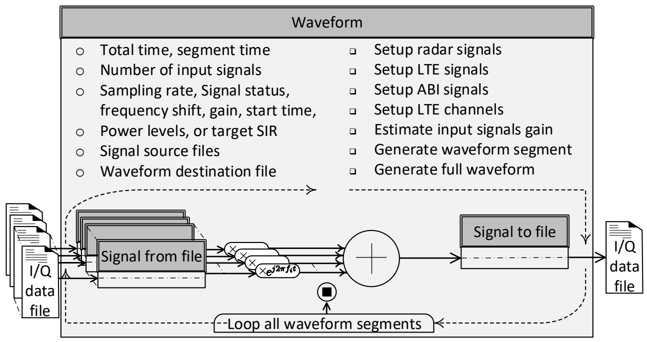

Figure 3: Test waveform generation

GUI utilizes the waveform generation framework to perform the generation process. The GUI allows up to two radar signals, two LTE signals and one ABI signal. The waveform parameters can be changed interactively in the preview mode to visualize the waveforms as shown in Fig. 4. In addition, the waveform generation panel simplifies the selection and randomization of the parameters [6]. The generated waveforms are 90 s long and sampled at 25 MHz.

5 ESC TEST HARNESS

5.1 Harness Overview

The test harness consists of two independent parts that run in realtime and a post processing portion that runs after the test is complete; a controller that manages the entire set of files (stored on a redundant array of independent disks, or RAID), and a player that plays a single waveform file at a time as issued by the controller. For auditing purposes the test harness also includes a recorder which digitally samples and records to a file the waveform being played as it is seen by the ESC sensor. A block diagram of the test harness is shown in Fig. 5.

The ESC test harness was implemented using a National Instruments (NI) PXIe chassis containing an NI vector signal transceiver (VST) to play the signals at RF, an NI vector signal analyzer (VSA) to record the signal being played, and an NI PC to act as the controller.[2] Also included in the setup is an RF splitter allowing the signal from the VST to go to both the ESC sensor as the unit under test and to the VSA/recorder. Additional hardware, such as a spectrum analyzer, can be used for realtime viewing of the waveform. This hardware can be seen in Fig. 6.

The ESC sensor connects to the test harness by an RF cable used to receive the signals sent by the test harness, and a network cable used by the ESC sensor to transmit detection messages to the test harness over HTTP.

[2]Certain commercial equipment, instruments, or materials are identified in this paper in order to specify the experimental procedure adequately. Such identification is not intended to imply recommendation or endorsement by the National Institute of Standards and Technology, nor is it intended to imply that the materials or equipment identified are necessarily the best available for the purpose.

5.2 Controller

The controller presents a web interface with a login page that prompts for credentials. After logging in, the user then inputs specific parameters for a manual test of a single waveform file or the filepath of a JavaScript Object Notation (JSON) file for an automated test of a batch of waveform files. In case of the latter, the controller takes this list of waveform files from the JSON file, issues them one at a time to the player, and waits for a response indicating completion of playback from the player. The controller also creates a new timestamped log file for the duration of the test batch. During playback, the controller is also listening for any messages from the ESC sensor; all such messages are timestamped and logged. The log file is used later in post-processing to generate performance metrics, as described in Section 5.5.

The test harness uses a single clock for reference, as supplied by the controller, to avoid the risk of clock drift when comparing events from the separate components of the test harness: controller, player, or the ESC sensor. The controller time-stamps the start of a waveform just prior to issuing it to the player, and time-stamps notifications it receives from the ESC sensor under test.

A possible timing hazard may arise from an ESC sensor that aggregates reporting data, for example every 60 s. The risk of this hazard is mitigated by ensuring that each test waveform exceeds 60 s. Furthermore, a delay can be inserted between consecutive test waveforms to reduce the likelihood that the response to one test waveform appears during playback of the next waveform.

5.3 RF Player Functionality and Operation

The RF player is the portion of the test harness that plays a single waveform file at a time over an RF cable, using the VST, to the ESC sensor. This is done by wrapping the player in a state machine to handle the metadata. The list of states is shown in Fig. 5.

The instruction to play a waveform file is received as a JSON message over a HTTP socket from the controller. This message tells the player both what file to play (by full filepath) and the metadata for how to play that file (i.e., baseband gain, RF gain, center frequency).

Once the player receives the JSON message from the controller, the player parses the message into its individual elements, conditionally converts the file to NI's technical data management solution (TDMS) format, and then generates the RF waveform to the ESC sensor under test. The player sends a message to the controller over HTTP to indicate that the file has finished playing. The player then proceeds to wait for the next message from the controller indicating which file to play next. This flow, implemented in NI LabVIEW software, is shown in Fig. 7.

If an error is experienced at any stage, the player proceeds to an error handling stage and reports back to the controller rather

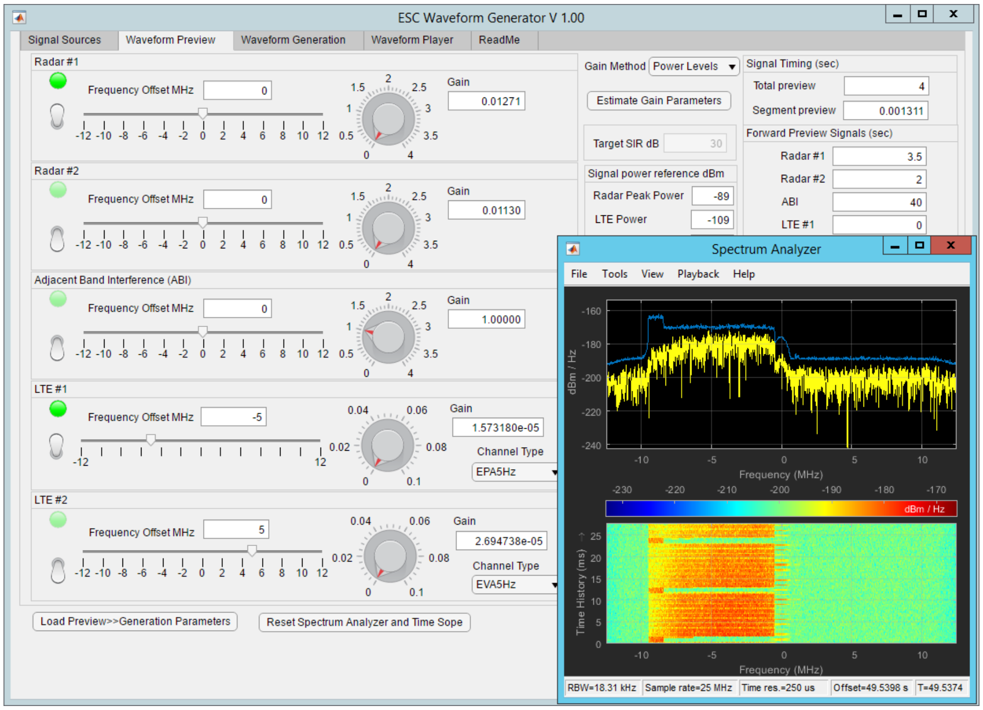

Figure 4: Preview panel of the waveform generator GUI

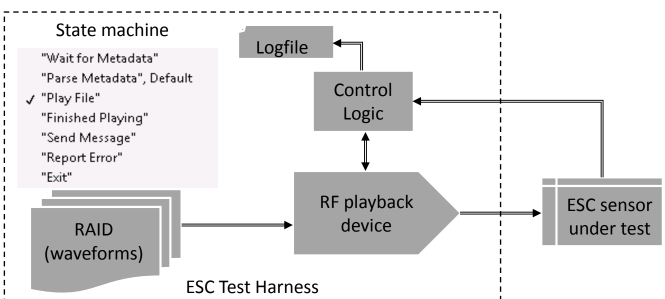

Figure 5: Block diagram and list of states for waveform player

than playing the file. This error handling is not shown in Fig. 7.

Fig. 8 expands the RF playback device block of Fig. 5 in more detail. The figure illustrates the hardware and software components associated with the RF playback subsystem, including the VST (NI 5646) and VSA (NI 5668). LabVIEW code implements NI RF Signal Generator (niRFSG) drivers which configure the VST as an arbitrary waveform generator (AWG) and a TDMS file reader, enabling the application to function as a waveform file player. The VST RF drivers configure parameters within the VST RF chain to enable signal generation at a specific center frequency, I/Q sampling rate, and RF output power.

The LabVIEW code also configures the first-in, first-out (FIFO) memory of the VST to be used as a buffer by the internal Virtex6 field programmable gate array (FPGA). Considering that the size of each waveform file is approximately 9 GB, which is significantly larger than the 1 GB on-board host VST dynamic

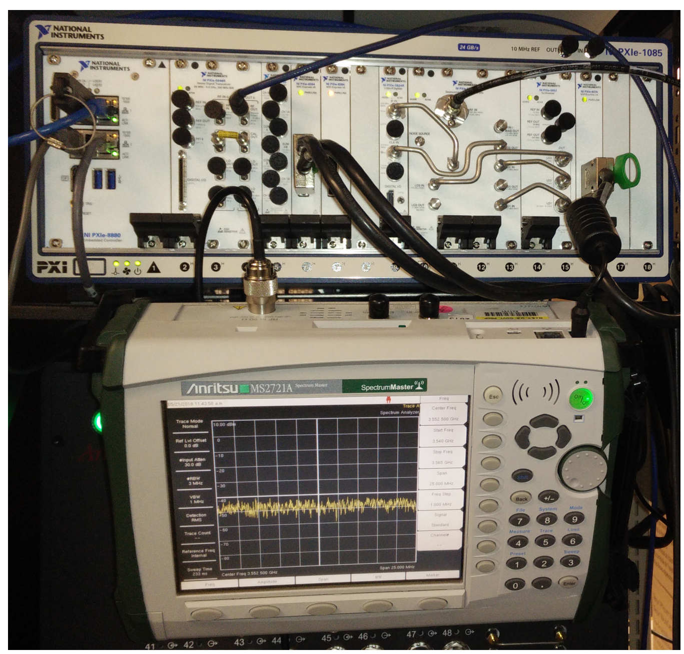

Figure 6: Photo of the hardware comprising the ESC test harness

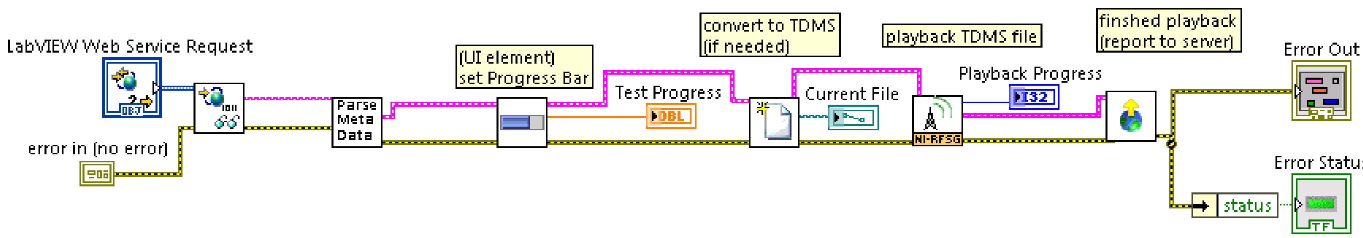

Figure 7: Block diagram of the RF player portion of the ESC test harness

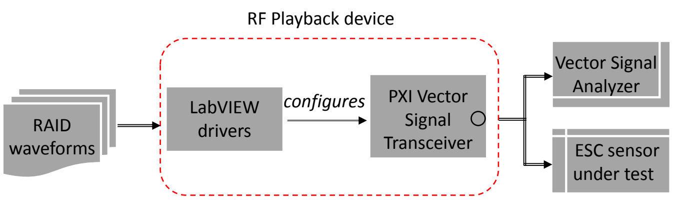

Figure 8: RF playback and record subsystem

random-access memory, it is necessary to process each waveform file in chunks. The configuration of the FPGA involves specifying the capacity, or depth, in elements of the FIFO. A direct memory access channel is formed between the FIFO buffer on the host VST and FPGA target enabling chunks of data to be transferred between the two nodes. As a result, the configuration allows for continuous data streaming of the TDMS waveform file for RF playback.

5.4 RF Power Correction

In order to generate the waveforms at desired power levels, the playback subsystem must be calibrated to compensate for cable loss and to correct for any other offsets in the RF chain. To calculate the correction, the cable losses were measured and added into the RF budget along with a correction factor derived from a custom test waveform file. The file contains five predefined tones with varying amplitudes at five different frequencies. An illustration of the tones is shown in Fig. 9. The correction factor which reproduced the tones at their expected amplitudes was then applied to the VST for playback of all waveform files.

5.5 Post-Processing of Detection Results

After the entire test is complete, the controller has generated a single timestamped log file. This logfile contains the start and end time of every portion of the test as reported by the player, as well as any messages received by the ESC sensor. All log entries are timestamped by the controller as they are written.

From the log file and the known characteristics, or ground truth, of each test waveform file (i.e., presence/absence of in-band radar, and its center frequency if present), a post-processing script can identify true detections, missed detections, false detections, and late detections. A true detection occurs when the waveform contains an in-band radar signal, and the ESC sensor under test correctly identifies the channel(s) on which it transmits. False detections occur when the ESC sensor reports a federal incumbent signal on a channel which contains no in-band radar signal. Late detections are a subset of correct detections where the radar was detected on the correct channel but not within 60 s of the time it first exceeded the detection threshold of $-89\,\mathrm{dBm/MHz}$.

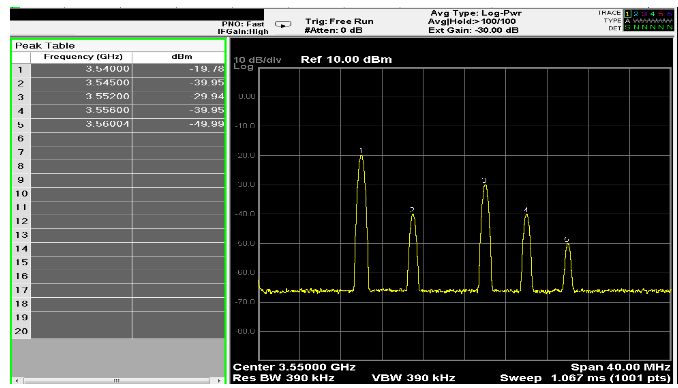

Figure 9: Multiple tones used to derive power correction

6 SAMPLE TEST SCENARIOS

To illustrate use of the test harness, we generated playback files with combinations of in-band radar and interference signals using the waveform generator tool described in Section 4. The generated waveforms were played consecutively using the ESC test harness described in Section 5. The waveforms were played with a $25\,\mathrm{MHz}$ sampling rate and $20\,\mathrm{MHz}$ bandwidth at $3.6\,\mathrm{GHz}$ and captured into a single I/Q file with the recorder as demonstrated in Fig. 10. For demonstration purposes, the waveform files were played at higher power levels than an actual test since the VSA in the absence of a preamplifier has a noise floor of $-150\,\mathrm{dBm/Hz}$. In an actual test, a preamplifier would be required to record these signals with a lower noise floor.

Six 90 s waveforms were played consecutively and recorded by the ESC test harness. From the recorded I/Q samples, a 6×90s spectrogram was generated with a max-hold of $0.2\,\mathrm{s}$

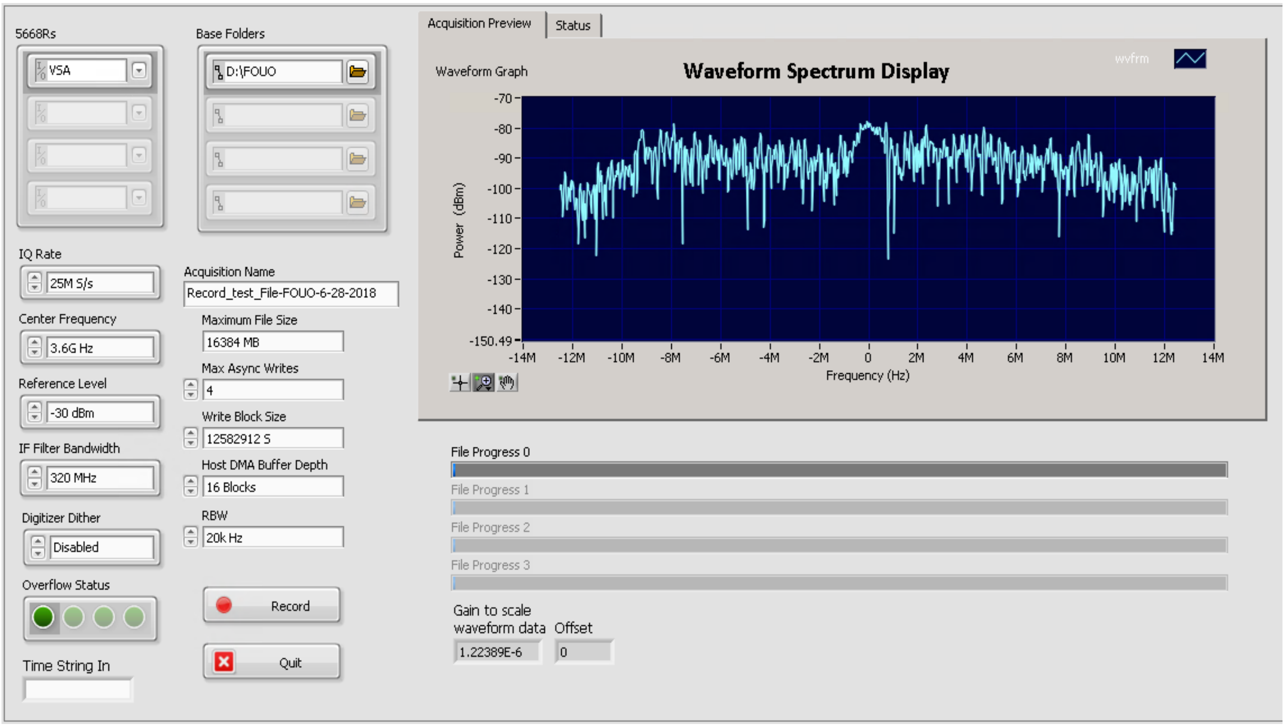

Figure 10: RF recorder

per spectral line. The remainder of this section briefly describes each 90 s portion of this test and presents a detection example of the incumbent radar signal over the entire recorded file.

6.1 In-band Radar

The first example shows a single in-band radar signal at a center frequency of 3.6 GHz. The radar signal starts after a delay of approximately 10 s and first rises above the detection threshold at approximately 13.4 s from the beginning of the waveform, as shown in Fig. 11. This case demonstrates a simple scenario where only one radar signal is present and no interference signal exists in the band.

6.2 Two Faded LTE Signals

The second portion of the test, shown in Fig. 12, demonstrates the presence of LTE signals when the in-band radar is absent. Two 10 MHz TDD LTE signals are assumed to be the dominant signals in their respective channels. The two LTE signals differ in terms of their TDD configurations and their up-link to down-link power ratios. In addition, time-varying multipath channel fading is applied to both signals.

6.3 In-band Radar with Co-Channel LTE

The next segment of the playback test shows an in-band radar signal co-channel with a fading LTE signal. As shown in Fig. 13, both the radar and the LTE signals are centered at 3.6 GHz. The radar signal in this waveform is relatively strong as shown in the time-domain plot of Fig. 14. The time-domain plot clearly shows the main-beam emission of the radar antenna as it sweeps past the receive antenna, as well as emissions from side lobes or strong reflections. Furthermore, the LTE signal envelope varies because of the channel fading.

6.4 In-Band Radar Between Two Faded LTE Signals

Fig. 15 shows a typical configuration with two LTE signals in adjacent channels and an in-band radar signal in the guard-band between the two channels. The radar signal is easily observable in this waveform since each LTE signal has a 9 MHz occupied bandwidth and is placed at ± 5 MHz from the radar center frequency.

6.5 Adjacent-Band Emissions

The segment of the test starting at 366 s and shown in Fig. 16 demonstrates interference from adjacent-band radar emissions. The in-band radar signal is absent and a robust ESC detector is expected to report no detection of in-band radar during this 90 s period. The adjacent-band emissions end approximately 60 s from the start of this segment since the original field-measured waveforms were 60 s in duration.

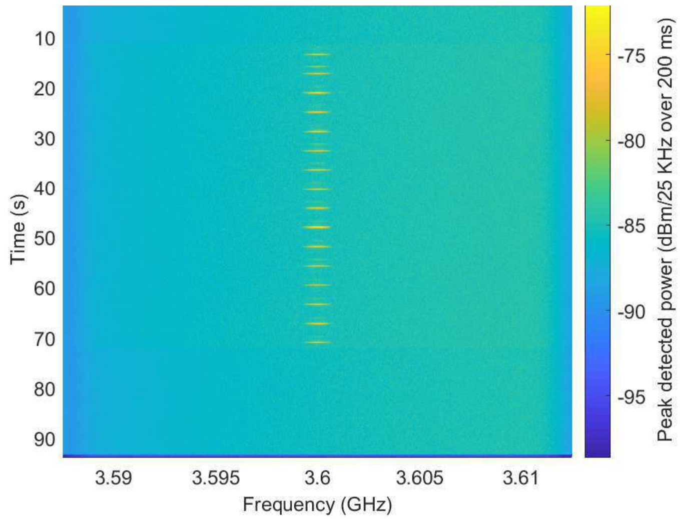

Figure 11: Spectrogram of in-band radar signal

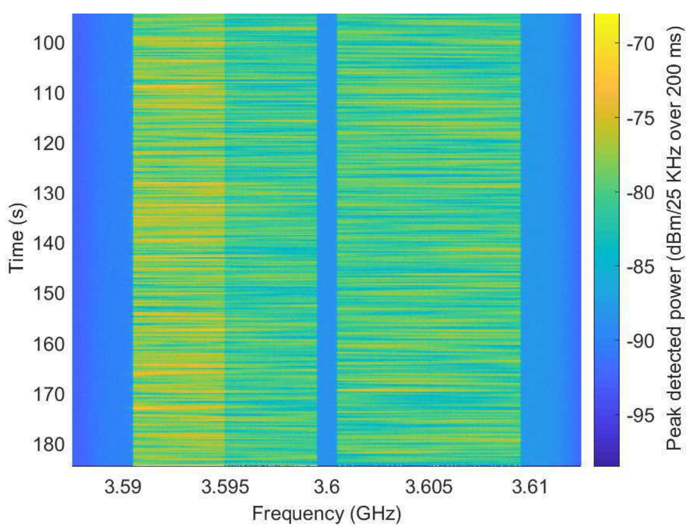

Figure 12: Spectrogram of two LTE signals with fading

6.6 Two In-Band Radars with Adjacent-Band Emissions

Finally, a more challenging scenario is shown in the last segment. As shown in Fig.17, two in-band radar signals are placed at center frequencies of 3.60 GHz and 3.61 GHz, respectively. In addition, the waveform contains adjacent-band interference. The two in-band radar signals start 28 s and 30 s into the generated waveform, respectively. The ESC detector is expected to detect both in-band radar signals during this portion of the test. Fig. 18 shows a time-domain plot of a 0.2 s slice of this segment during which the main beam of one of the in-band radars sweeps past the receiver; the stronger peaks are adjacent-band emissions.

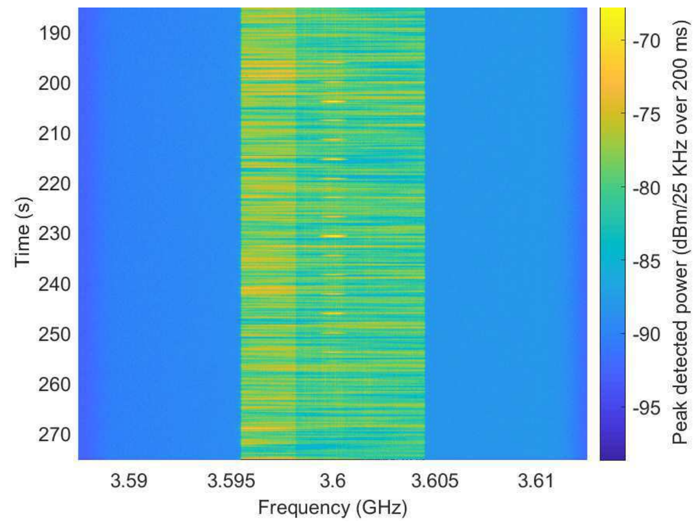

Figure 13: Spectrogram of in-band radar signal with co-channel LTE

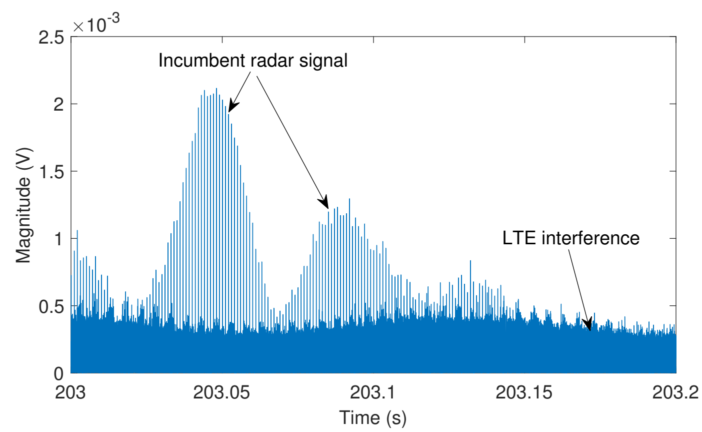

Figure 14: Time-domain plot of a 0.2 s portion of the in-band radar signal with co-channel LTE (at the 203 s mark of the test)

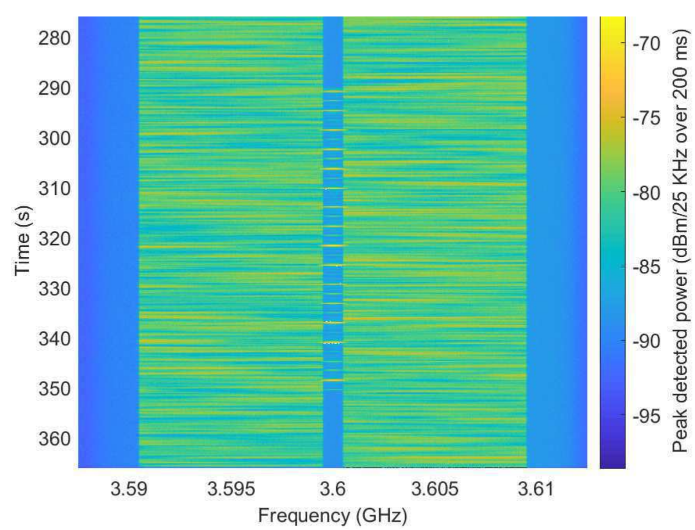

Figure 15: Spectrogram of in-band radar signal between two fading LTE signals

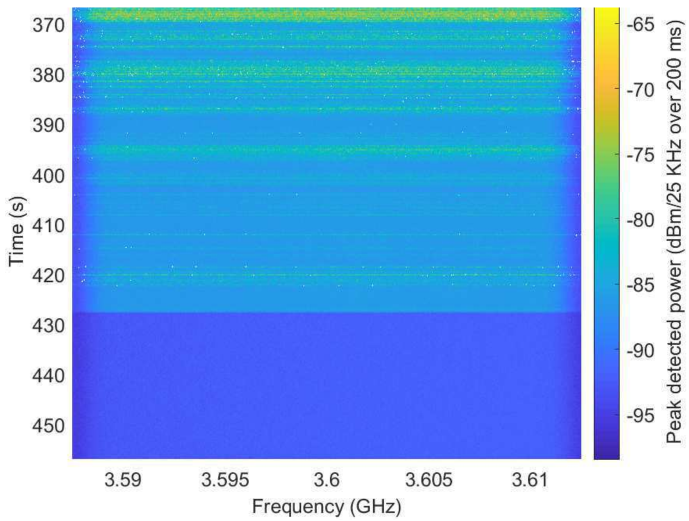

Figure 16: Spectrogram of adjacent-band interference

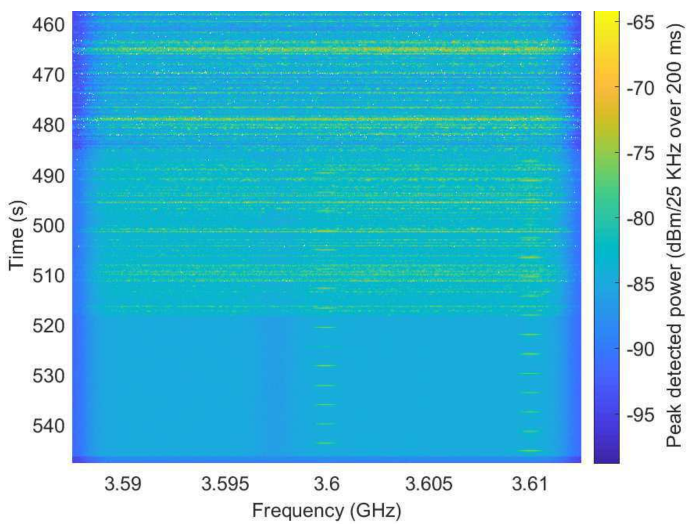

Figure 17: Spectrogram of two in-band radar signals with adjacent-band interference

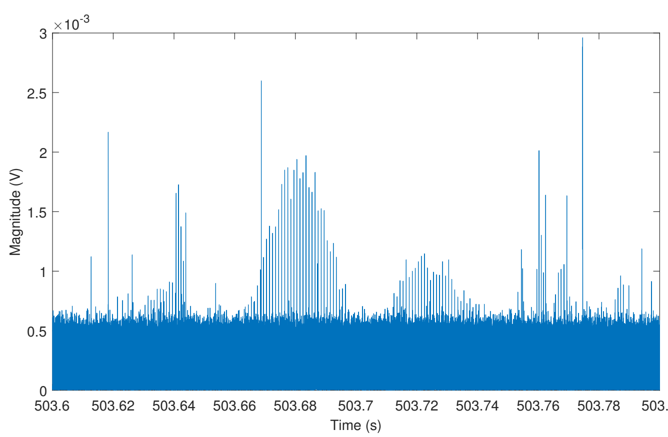

Figure 18: Time-domain plot of a 0.2 s portion of the two in-band radar signals with adjacent-band interference (at the 503.6 s mark of the test)

6.7 Detection Example

In addition to off-line verification of the test signal, the recorded file from the ESC test harness can be used to evaluate a detection algorithm by simulation. To demonstrate, we fed the recorded sequence of waveforms to a matched-filter detector matched to the currently deployed in-band radar signal and centered at 3.6 GHz. The matched filter uses a 10 ms synthetically generated pulse burst with a pulse repetition time of 1 ms and a pulse width of 1 µs, similar to the one presented in [8]. Fig. 19 shows the output of the detector versus test time. The peak values at the output of the detector are proportional to the received signal amplitude, and most correspond to sweeps of the main beam of the radar antenna. The detector output accurately reflects the presence of the in-band radar signal at 3.6 GHz as the test time advances. A threshold can be applied at the output of the detector to decide whether an in-band radar signal is present or absent at this frequency. The threshold value shown in Fig. 19 is for demonstration only.

7 SUMMARY

This paper presented a framework and apparatus for quantitatively assessing the performance of a 3.5 GHz ESC sensor using test signals comprised of field-measured and synthetically generated waveforms. Test signals are generated prior to the test for a variety of commercial-federal signal scenarios in which the relative amplitudes and frequency offsets of all signal components can be varied. A test harness automates the test process by generating a script of RF test signals and logging sensor detections. It can also record the test signals as they are seen by the sensor under test for auditing purposes. Following the test, test scripts and test logs can be processed to generate sensor performance metrics such as detection and false alarm rates.

The paper concludes with a series of example scenarios generated by the test apparatus to illustrate its flexibility and expected uses. Further work can incorporate the signals of federal incumbent systems yet to be deployed in the band and which the sensors are expected to detect.

REFERENCES

[1] "Citizens broadband radio service," 2 C.F.R. § 96, 2016.

[2] F. H. Sanders, J. E. Carroll, G. A. Sanders, R. L. Sole, J. S. Devereux, and E. F. Drocella, "Procedures for laboratory testing of environmental sensing capability sensor devices," National Telecommunications and Information Administration, Technical Memorandum TM 18-527, Nov. 2017. [Online]. Available: http://www.its.bldrdoc.gov/publications/3184.aspx

[3] "Requirements for commercial operation in the U.S. 3550–3700 MHz citizens broadband radio service band," Wireless Innovation Forum Document WINNF-TS-0112, Version V1.5.0, May 2018. [Online]. Available: https://workspace.winnforum.org/higherlogic/ws/public/document?document_id=6531

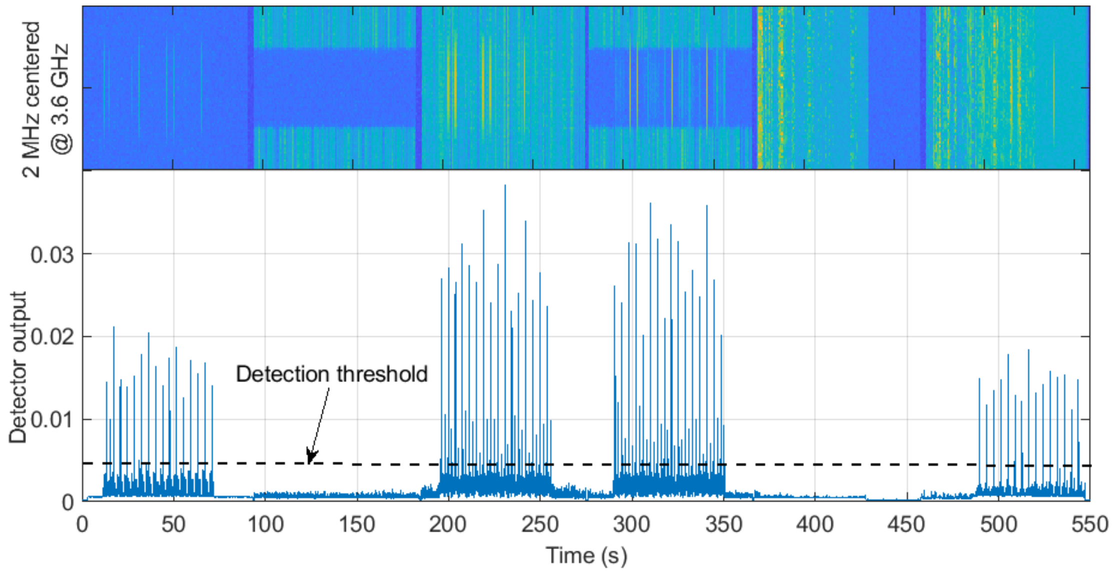

Figure 19: Response of in-band radar matched filter to the recorded test waveform

[4] P. D. Hale, J. A. Jargon, P. J. Jeavons, M. R. Souryal, A. J. Wunderlich, and M. Lofquist, “3.5 GHz radar waveform capture at Point Loma: Final test report,” National Institute of Standards and Technology, Technical Note 1954, May 2017. [Online]. Available: https://www.nist.gov/publications/35-ghz-radar-waveform-capture-point-loma

[5] P. D. Hale, J. A. Jargon, P. J. Jeavons, M. R. Souryal, A. J. Wunderlich, and M. Lofquist, “3.5 GHz radar waveform capture at Fort Story: Final test report,” National Institute of Standards and Technology, Technical Note 1967, Aug. 2017. [Online]. Available: https://www.nist.gov/publications/35-ghz-radar-waveform-capture-fort-story-final-test-report

[6] R. Caromi, J. Mink, and M. Souryal, “3.5 GHz waveform generation for testing and development of ESC detectors,” WInnComm, San Diego, Nov. 2017.

[7] R. Caromi, J. Mink, and M. Souryal, “3.5 GHz waveform generation for testing and development of ESC detectors,” https://github.com/usnistgov/ESCWaveformGenerator, 2017.

[8] R. Caromi, M. Souryal, and W. Yang, “Detection of incumbent radar in the 3.5 GHz CBRS band,” in *Proc. IEEE GlobalSIP*, Nov. 2018.